Molecular Vision 2014; 20:1002-1016 <http://www.molvis.org/molvis/v20/1002>
Received 30 January 2014 | Accepted 3 July 2014 | Published 7 July 2014

© 2014 Molecular Vision

Comparison of effect of gamma ray irradiation on wild-type and N-terminal mutants of αA-crystallin

Srinivasagan Ramkumar,[1] Noriko Fujii,[2] Norihiko Fujii,[2,3] Bency Thankappan,[1] Hiroaki Sakaue,[2] Kim Ingu,[2] Kalimuthusamy Natarajaseenivasan,[4] Kumarasamy Anbarasu[1]

[1]Department of Marine Biotechnology, Bharathidasan University, Tiruchirappalli, Tamil Nadu, India; [2]Research Reactor Institute, Kyoto University, Kumatori-cho, Sennan-gun, Osaka, Japan; [3]Teikyo University, Japan; [4]Department of Microbiology, Bharathidasan University, Tiruchirappalli, Tamil Nadu, India

Purpose: To study the comparative structural and functional changes between wild-type (wt) and N-terminal congenital cataract causing αA-crystallin mutants (R12C, R21L, R49C, and R54C) upon exposure to different dosages of gamma rays.

Methods: Alpha A crystallin N-terminal mutants were created with the site-directed mutagenesis method. The recombinantly overexpressed and purified wt and mutant proteins were used for further studies. A ^{60}Co source was used to generate gamma rays to irradiate wild and mutant proteins at dosages of 0.5, 1.0, and 2.0 kGy. The biophysical property of the gamma irradiated (GI) and non-gamma irradiated (NGI) αA-crystallin wt and N-terminal mutants were determined. Oligomeric size was determined by size exclusion high-performance liquid chromatography (HPLC), the secondary structure with circular dichroism (CD) spectrometry, conformation of proteins with surface hydrophobicity, and the functional characterization were determined regarding chaperone activity using the alcohol dehydrogenase (ADH) aggregation assay.

Results: αA-crystallin N-terminal mutants formed high molecular weight (HMW) cross-linked products as well as aggregates when exposed to GI compared to the NGI wt counterparts. Furthermore, all mutants exhibited changed β-sheet and random coil structure. The GI mutants demonstrated decreased surface hydrophobicity when compared to αA-crystallin wt at 0, 1.0, and 1.5 kGy; however, at 2.0 kGy a drastic increase in hydrophobicity was observed only in the mutant R54C, not the wt. In contrast, chaperone activity toward ADH was gradually elevated at the minimum level in all GI mutants, and significant elevation was observed in the R12C mutant.

Conclusions: Our findings suggest that the N-terminal mutants of αA-crystallin are structurally and functionally more sensitive to GI when compared to their NGI counterparts and wt. Protein oxidation as a result of gamma irradiation drives the protein to cross-link and aggregate culminating in cataract formation.

The human lens is composed of a unique protein known as crystallin, which is endowed with high stability and durability. Crystallin is categorized as α, β, and γ based on genetic organization and expression pattern [1]. α-crystallin predominates in the eye lens (about 40% to 50% of the total) and is composed of two subunits, namely, αA and αB-crystallin. The chaperone-like function of α-crystallin plays a critical role in maintaining lens transparency by preventing the aggregation of unfolded proteins and cellular damage [2-4].

Cataract is defined as opacification of the eye lens associated with the breakdown of the lens microarchitecture that impairs vision [5]. Congenital or pediatric cataract appears during birth or within the first year of life and is the most common cause of childhood blindness, which has 30% to 50% of genetic basis [6-8]. Others are intrauterine infections, uptake of drug or radiation in pregnancy, gene defects, chromosomal disorders, metabolic disease, trauma, etc. [9]. Approximately 70% of lens opacification in congenital cataract is due to anomalies in the lens alone [10]; the remaining opacification includes ocular anomalies such as microphthalmia, aniridia, other anterior chamber developmental anomalies, or retinal degeneration [11].

Mutation in the evolutionarily conserved amino acids in the N-terminal domain of the human αA-crystallin gene provokes the formation of congenital cataract. Few such mutations were considered for this investigation. The human αA-crystallin consists of a conserved central domain flanked by N- and C-terminal domains confirmed to play an important role in oligomerization [12,13]. Four congenital cataract-causing mutants in the region of the N-terminal have been predominantly reported, R12C [6,13], R21L [14], R49C [15], and R54C [6], worldwide. These mutant-affected members had autosomal dominant bilateral congenital nuclear cataract unveiled to possess mutation in the arginine residue. The deleterious effect on the mutational conversion of arginine

Correspondence to: K. Anbarasu, Department of Marine Biotechnology, Bharathidasan University, Tiruchirappalli – 620 024, Tamil Nadu, India; Phone: +91 431 2407071 Etn: 436; FAX: +91 431 2407045; email: anbumbt@bdu.ac.in

reveals the crucial role of arginine in either substrate binding or protein structure stabilization thus influencing the chaperone-like activity. Most congenital mutations are mutated in the arginine residues, forming either cysteine, leucine, tryptophan, or histidine [16] in the eye lens αA and αB-crystallins. Modeling studies performed by Ijssell et al. [17] on sHSP 16.5 of *Methanococcus janaschii* demonstrated that the arginine residue (position 107) is buried in the hydrophobic core of the protein and forms a salt bridge with glycine. Bera et al. [18], in extensive structural and functional studies in the mutant R116C, reported the loss of the positive charge on the mutation in αA-crystallin that is crucial for forming salt bridges with neighboring negatively charged residues, eventually leading to protein unfolding and aggregation. Further, extensive studies have been performed to determine the structural and functional perturbation of the N-terminal mutants of αA-crystallin proteins using the recombinant approach [16,19,20], which has contributed to unraveling the mechanism of cataractogenesis.

It has been previously reported that the morphology of cataract has some correlation with the expression pattern of the mutated protein. However, varying morphologies and severities of the disease have been observed with the same mutation in different families and even within the same family suggesting the involvement of other environmental factors in the magnitude of the disease [11]. Gamma ray–induced modification of the structural and functional properties of αA-crystallin has been performed mimicking the physiologic stress condition. However, to the best of our knowledge, there are no reports on the effect of such stress on N-terminal mutants of αA-crystallin proteins. It is crucial because proteins including the mutant forms in a cell are prone to various oxidative stresses under physiologic conditions [21]. Constant exposure to oxidative stress, environmental elements, metabolic disorders, and genetic variations contributes to the pathomechanism of the early onset of cataract development. Apart from oxidative stress, mutations, truncations, deamidations and glycation plays a crucial role in the pathophysiology of cataractogenesis resulting in changes in the epithelial cell metabolism, lenticular protein structure, and function that are elusive [22]. Gamma irradiation (GI)–induced oxidation in the lens closely imitates the modifications that occur in cataract formation during aging [23]. Our previous studies demonstrate that gamma rays induce oxidation in bovine αA-crystallin evoking isomerization of Asp151, cross-link product formation, oxidation of methionine 1, and decreased chaperone activity [24]. Thus, to understand the structural and functional behavior of the αA-crystallin N-terminal mutant proteins as a result of oxidative stress when compared to the native αA-crystallin, we adopted gamma rays as a medium for generating oxidative stress for the mutants, and the structural and functional perturbation of the mutant proteins were analyzed.

METHODS

Site-directed mutagenesis: The αA-crystallin N-terminal mutants, R12C, R21L, R49C, and R54C, were created by site-directed mutagenesis using the following primers: 5′-TGG TTC AAG **T**GC ACC CTG GGG-3′ (forward), 5′-CCC CAG GGT GC**A** CTT GAA CCA-3′ (reverse) for R12C; 5′-TTC TAC CCC AGC C**T**G CTG TTC GAC-3′ (forward), 5′-GTC GAA CAG C**A**G GCT GGG GTA GAA-3′ (reverse) for R21L; 5′-CCC TAC TAC **T**GC CAG TCC CTC T-3′ (forward), 5′-AGA GGG ACT GGC **A**GT AGT AGG G-3′ (reverse) for R49C; and 5′-TCC CTC TTC **T**GC ACC GTG CTG-3′ (forward), 5′-CAG CAG GGT GC**A** GAA GAG GGA-3′ (reverse) for R54C. The primers, designed manually by replacing a single nucleotide at the middle of the primer sequence and custom synthesized at Bioserve Biotechnologies (Hyderabad, India), have cysteine and leucine in the place of the arginine codon. The cDNA construct of αA-crystallin wt in pET 3d [23] was used as the template for generating the mutants using the Quick Change II XL site-directed mutagenesis kit (Agilent Technologies, Santa Clara, CA) following the manufacturer's protocol. PCR amplification was performed with an initial denaturation of 95 °C for 1 min, followed by 16 cycles of 95 °C for 50 s, 60 °C for 50 s, and 68 °C for 5 min followed by an overall extension at 68 °C for 7 min. The amplicons were digested with *Dpn*I for 1 h at 37 °C, and the products were transformed into XL-10 Gold competent *Escherichia coli* cells. The transformed cells were selected on Luria bertani broth (LB) agar plates containing 50 µg/ml ampicillin. The mutant constructs were validated with restriction digestion and DNA sequence analysis.

Overexpression and purification of protein: Human αA-crystallin wt and N-terminal mutants in pET 3d vector were transformed into *E. coli* BL21 (DE3) pLysS cells. Protein production was induced in the cultured cells with the addition of isopropyl-1-thio-β-d-galactopyranoside (IPTG) induction to a final concentration of 0.3 mM. The cells were subsequently thawed, sonicated (six rounds of 8 pulses per minute) in 20 mM Tris-HCl, pH 7.8 containing 1 mM ethylenediamine tetraacetic acid (EDTA) and 1 mM phenyl methanesulfonyl fluoride (PMSF). The sonicated products were centrifuged at 48850 ×g for 20 min, and the soluble fraction was subject to ion exchange column chromatography on a Q Sepharose XL column (Amersham Biosciences, Piscataway, NJ) equilibrated with 20 mM Tris-HCl containing 1 mM EDTA and connected to an AKTA prime plus (GE

Healthcare, Buckingham Shire, UK). The protein was eluted using a gradient of 0–1 M NaCl with a flow rate of 10 ml/min. The αA-crystallin wt and mutants were eluted at 300 mM NaCl. The purified αA-crystallin wt and mutant samples were further purified on a size exclusion column (Sephacryl 300HR; Amersham Biosciences) equilibrated with 20 mM Tris-HCl pH 7.8 containing 150 mM NaCl. The purity of the recombinant protein was checked with 15% sodium dodecyl sulfate–polyacrylamide gel electrophoresis (SDS–PAGE) and western blotting. The purified αA-crystallin wt and its N-terminal mutants were dialyzed against 50 mM sodium phosphate buffer (pH 7.8) for further biophysical experiments.

Western blotting: Proteins separated using 15% SDS–PAGE were transferred onto nitrocellulose membrane at 12 V for 1 h using a semidry western blotting system (Bio-Rad, Hercules, CA). The membrane was blocked for 1 h at room temperature in Tris buffer saline with 0.1% Tween-20 (TBS-T) containing 3% (w/v) skimmed milk powder. After three washes with TBS/T of 5 min each, the membrane was incubated with polyclonal anti-αA-crystallin antibody FL-173 (Santa Cruz Biotechnology, Dallas, TX, FL-173) at a dilution of 1:1,000 overnight at 4 °C. After washing, the membrane was incubated for 1 h with anti-rabbit immunoglobulin G (IgG) conjugated to alkaline phosphatase (Sigma, St. Louis, MO) at a dilution of 1:10,000. The membrane was washed again, and the blots were developed with the bromo-4-chloro-3-idolyl phosphate/nitroblue tetrazolium chloride (BCIP/NPT) substrate (Sigma).

Gamma irradiation of αA-crystallin and congenital cataract causing N-terminal mutants: To investigate the effect of GI on the αA-crystallin wt and N-terminal mutants, aliquots of 1 mg/ml protein in 50 mM sodium phosphate buffer (pH 7.8) were exposed to gamma radiation doses (0.5, 1.0, and 2.0 kGy) at a rate of 509 Gy/h from a ^{60}Co source at the Research Reactor Institute, Kyoto University (Kyoto, Japan).

The profile of the GI αA-crystallin (wt and mutant) was examined with 15% SDS–PAGE at pH 8.8 according to the standard method [25]. The gels were stained with Coomassie brilliant blue (R250), destained and high molecular weight (HMW) cross-linked product formation of GI αA-crystallin compared to the NGI samples.

Size exclusion chromatography: The molecular mass difference between the GI and NGI αA-crystallin wt and the congenital N-terminal mutant samples was ascertained with size exclusion chromatography on a TSKgel-G4000SWXL column (7.8 × 300 mm, Tosho, Tokyo, Japan). The column was equilibrated in 50 mM Tris-HCl containing 150 mM NaCl with a flow rate of 0.8 ml/min. About 100 µl of the 1 mg/ml experimental protein was injected onto the column, and the elution protein profile was recorded with absorbance detection at 280 nm. Molecular masses were acquired by calibrating the column with molecular mass standards.

Circular dichroism: A circular dichroism (CD) spectropolarimeter (Jasco 810, Kyoto, Japan) was used to record the CD spectra of the GI and NGI αA-crystallin wt and N-terminal mutants. Far-ultraviolet (UV) CD measurements were performed between wavelengths of 195 to 250 nm at room temperature. Scans were performed using a cylindrical quartz cuvette with a 1 mm path length. Protein samples of 0.1 mg/ml were prepared in 50 mM sodium phosphate buffer (pH 7.8). Spectra represented are the average of five scans. The buffer signal was subtracted and smoothed.

Surface hydrophobicity: The relative surface hydrophobicity of the GI and NGI αA-crystallin wt and N-terminal mutants were determined with 4,4'-bis(1-anilinonaphthalene 8-sulfonate) (bis-ANS), a hydrophobic probe, as described previously [23]. Briefly, an aliquot of 100 µl of bis-ANS (0.1 mg/ml) was added to 100 µl of protein (1 mg/ml) along with 800 µl of 50 mM sodium phosphate buffer (pH 7.8). Before the experiment, the reaction mixtures were incubated at room temperature for 15 min in the dark. The intensity of the fluorescence was measured using an F-4500 Hitachi fluorescence spectrophotometer (Hitachi, Tokyo, Japan) with excitation of 390 nm and emission at 420–560 nm.

Chaperone activity: Chaperone activities of the GI and NGI αA-crystallin wt and N-terminal mutants were measured via the ability of crystallin to protect against the aggregation of alcohol dehydrogenase (ADH) induced by EDTA with αA-crystallin and ADH in a 1:5 ratio (w/w). An aliquot (500 µl) of 0.5 mg/ml ADH and 350 µl of 50 mM sodium phosphate buffer (pH 7.2) containing 100 mM NaCl were incubated for 30 min at 37 °C with 50 µl of 1.0 mg/ml GI or NGI αA-crystallin wt and N-terminal mutants. ADH aggregation was initiated by adding 100 µl of 100 mM EDTA to each of the incubated reaction mixtures in a thermostat holder, and light scattering monitored for 60 min at 360 nm with a ultraviolet-visible (UV-Vis) spectrophotometer with a thermostat controller (Shimadzu UV-1200, Kyoto, Japan). The data were statistically analyzed with one-way ANOVA using SPSS software version 16 (Chicago, IL), and significance was considered at the level of *$p<0.05$ and *** $p<0.01$.

RESULTS

Confirmation of αA-crystallin mutants: The point mutants, created by site-directed mutagenesis and preliminarily confirmed with DNA double-digestion, are shown in Figure 1A demonstrating clear and distinct bands at approximately 512 bp and 4.6 kb on a 2% agarose gel, confirming the

presence of the insert and the vector, respectively. Further, Figure 2 shows the confirmation and comparison of the undigested plasmid and double-digested clones harboring the mutants R12C, R21L, R49C, and R54C. Figure 1B shows the chromatogram of the clones obtained as a result of sequencing. The mutated sequence in the chromatogram of the clones, R12C, R21L, R49C, and R54C, was analyzed and confirmed.

Purification of αA-crystallin and N-terminal mutants: The sodium dodecyl sulfate–polyacrylamide gel electrophoresis (SDS–PAGE) results demonstrate a level of purity of the eluted proteins of more than 95% (Figure 1C), which was further confirmed with western blotting (Figure 1D). The blotting results show the appearance of insoluble dark blue diformazan precipitate thus confirming the presence of αA-crystallin and mutants.

Radiolysis-induced formation of cross-linked products: Figure 3 indicates a decrease in monomeric forms and an increase in cross-linked product formation in all N-terminal mutants as the gamma rays dosage increased, when compared to the wild-type and NGI counterparts. αA-crystallin wt showed a decrease in the monomeric form and slightly increased higher cross-linked product formation at 2.0 kGy. However, the mutants R21L and R54C exhibited a drastic decrease in the monomeric form and increased high molecular weight (HMW) cross-linked product formation at all dosages of GI. The mutants R12C and R49C demonstrated a decrease in the monomeric form, and increased HMW cross-linked products started to be detectable upon exposure to 1.0 kGy and above with a significant level at 2.0 kGy of GI. The αA-crystallin wt and the N-terminal mutants formed HMW cross-linked products due to GI, but the level of product formation was higher in the mutants compared to the wt and NGI mutants. In a nutshell, all mutants started to form cross-linked product at a minimal dosage of 0.5 kGy; nevertheless, in αA-crystallin wt, the first sign of a significant level of increased cross-linked product formation was observed only at 2.0 kGy of GI. The densitometric analysis also confirmed the diminishing level of monomeric form due to GI in the N-terminal mutants analyzed with ImageJ software (Figure 4).

Increased aggregation of crystallin mutants on gamma irradiation: Figure 5A–C shows no significant changes in the elution profile of the NGI and GI αA-crystallin wt up to 1.0 kGy. Moreover, at the lower irradiation dosage of 0.5 kGy the elution profile of the NGI and GI αA-crystallin wt and N-terminal mutants were comparable. However, the elution peaks of the N-terminal mutants R12C, R49C, and R54C at 1.0 kGy appeared earlier than the control, demonstrating an increased size due to protein aggregation. Furthermore, at 2.0 kGy the mutant proteins elution profile was near the void volume corresponding to an apparent molecular mass of >7 × 10^6 Da (Figure 5D). The R21L mutant showed an increased aggregate size only at 2.0 kGy of gamma irradiation. Thus, it can be concluded that the recombinant αA-crystallin wt appears stable to GI whereas the N-terminal mutants started forming aggregation products from 1.0 kGy. Thus, mutation in arginine to cysteine conversion enhances cross-linked product formation when compared to the leucine conversion as well as the formation of disulfide bond between intra- or inter-polypeptide.

Gamma-irradiated mutants display changes in secondary structure: Far-UV spectra indicated that gamma irradiation of mutant proteins perturbed the secondary structure (Figure 6). The NGI αA-crystallin wt and N-terminal mutants almost retained their secondary structure without many changes, and a slight change was observed only in the R54C. Similarly, the αA-crystallin wt retained its secondary structure even at 2.0 kGy of GI (Figure 6A–D). In contrast, GI altered the β-sheet content and increased the random coil structure after 0.5 kGy in all N-terminal mutants. The greatest change in the β-sheet and random coil structure was observed in the mutants R12C, R21L, and R49C after 0.5 kGy exposure whereas the R54C mutant exhibited only slight changes in the β-sheet structure. We found that the degree of change or increase was directly proportional to the irradiation dosage and the location of the point mutation; the higher GI dosage resulted in greater perturbation in the secondary structure of the αA-crystallin N-terminal mutants. At 2.0 kGy, a drastic perturbation of the secondary structure was observed for all mutant proteins (Figure 6D).

Non-uniformity of surface hydrophobicity exposure among mutants: Figure 7 shows the bis-ANS fluorescence intensity of the NGI and GI αA-crystallin wt and N-terminal mutants. At 0, 0.5, and 1.0 kGy, all the mutants exhibited decreased surface hydrophobicity when compared to the αA-crystallin wt (Figure 7A–C). At 1.0 kGy, when compared to the NGI counterparts, the αA-crystallin wt and the mutant R12C exhibited a considerable decrease in surface hydrophobicity. Unexpectedly, R54C demonstrated a sudden increase in surface hydrophobicity at 2.0 kGy, and αA-crystallin wt, R21C, and R49C did not show any changes in fluorescence. However, a slight decrease in surface hydrophobicity was observed in the mutant R21L (Figure 7D).

Irradiated mutants exhibit increased chaperone activity: The chaperone function of the GI and NGI αA-crystallin wt and mutant proteins was determined using the client protein alcohol dehyderogenase (ADH). The chaperone activity of the αA-crystallin wt was slightly decreased after GI (Figure 8).

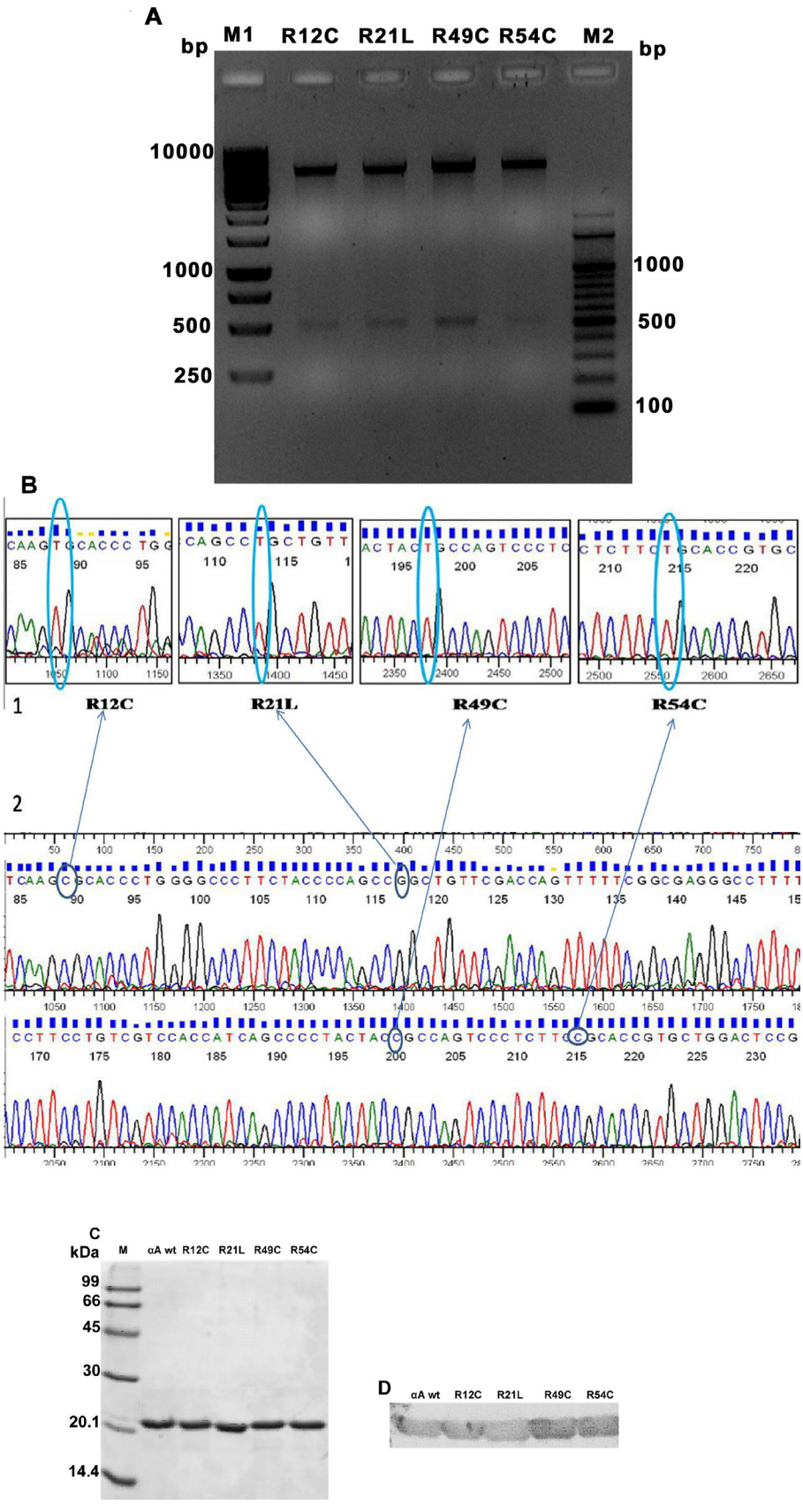

Figure 1. Confirmation of recombinant αA-crystallin wild-type and mutants. **A**: The 2% agarose gel electrophoresis image shows confirmation of clones by DNA double-digestion using the restriction enzymes *Nco*I and BamHI. The double-digested products show two individual bands approximately 4.6 kb and 512 bp representing the vector and the insert, respectively. Lanes 2–5 denote the doubly digested product of R12C, R21L, R49C, and R54C, respectively. M1 is the 100 bp DNA ladder and M2 1 kb DNA ladder. **B**: The boxed chromatogram represents the site-directed mutation at the specific points (circled) in the αA-crystallin gene. The circle represents the change in the nucleotide that creates N-terminal crystallin mutants such as R12C, R21L, R49C, and R54C. The second chromatogram represents αA-crystallin wild-type (wt). **C**–**D**: Sodium dodecyl sulfate–polyacrylamide gel electrophoresis (SDS–PAGE) and western blotting, respectively, of the αA-crystallin wt and N-terminal mutants. The purified αA-crystallin wt and N-terminal mutants (R12C, R21L, R49C, and R54C) were separated by 15% SDS–PAGE and transferred on to the nitrocellulose membrane for blotting. The blot was probed with human anti-αA-crystallin antibody, followed by secondary anti-rabbit immunoglobulin G (IgG) antibody conjugated to alkaline phosphatase. The blot was developed by adding the 5-Bromo-4-Chloro-3-idolyl Phosphate / Nitroblue tetrazolium chloride (BCIP/NBT) substrate. The appearance of insoluble dark blue diformazan precipitate in the blot confirmed the presence of αA-crystallin.

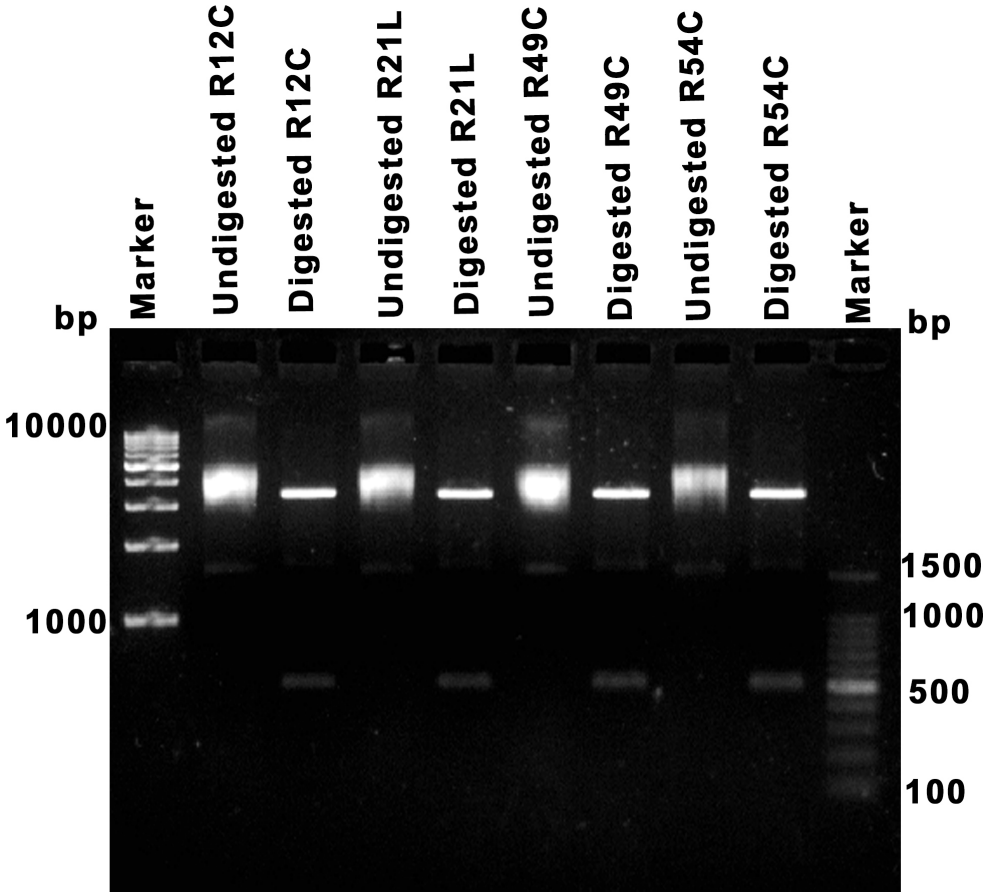

Figure 2. Confirmation of clones by double-digestion. The 2% agarose gel electrophoresis image shows confirmation of clones by DNA double-digestion using the restriction enzymes *Nco*I and BamHI. Lanes 2, 4, 6, and 8 represent the undigested plasmid of the clones R12C, R21L, R49C, and R54C mutants. Lanes 3, 5, 7, and 9 denote the double-digested products of the R12C, R21L, R49C, and R54C mutants. The release of the insert on double-digestion was confirmed by the appearance of a distinct band at approximately 512 bp.

The chaperone activity for all mutants irradiated with gamma rays against ADH as the substrate is given in Table 1 in terms of percentage. Notably, all GI N-terminal mutants exhibited an increase in chaperone activity compared to the NGI mutant counterparts as observed by the increasing suppression of ADH aggregation. As shown in Table 1, at 0 kGy the αA-crystallin wt showed 92% of chaperone activity; however, the mutants R12C, R21L, R49C, and R54C exhibited only 46.7%, 72.3%, 87.8%, and 78% of chaperone activity, respectively. Nevertheless, at 0.5 kGy GI all mutants, R12C, R21L, R49C, and R54C exhibited a slight increase in chaperone activity of 61.4%, 84.8%, 93.5%, and 83.6%, respectively, whereas the αA-crystallin wt showed s non-significant meager loss in its chaperone activity, exhibiting 91.3%. At 1.0 and 2.0 kGy, the αA-crystallin wt demonstrated 89.2% and 87.9% of chaperone activity, respectively; however, all mutants showed increased chaperone activity. R12C, R21L, R49C, and R54C exhibited 73.2%, 89.8%, 95.9%, and 85.7% of chaperone activity, respectively, at 1.0 kGy, and at 2.0 kGy, the rates were 80.1%, 92.1%, 97.4%, and 88.7%, respectively. The results clearly indicate the significance of the arginine residue in the N-terminal domain of αA-crystallin, and GI changed the chaperone function in the wt and mutants. Moreover, the arginine residues play a vital role in chaperone activity. The increased chaperone activity of the GI N-terminal mutants may be due to changes in hydrophobicity, the increased number and position of cysteine residues, the involvement of disulfide linkage formation, covalent protein–protein interaction, substrate binding potential, etc.

DISCUSSION

αA-crystallin wt is reported to be more resistant to the effects of gamma ray–induced oxidative damage than αB-wt [23]. Of the various post-translational modifications reported previously [26-32], oxidation of αA-crystallin leads to altered biophysical properties such as oligomerization, secondary structure, chaperone activity, and hydrophobicity of the protein. Gamma rays have the ability to induce reactive oxygen species (ROS) production in aqueous solution and thus can result in oxidization of the first αA-crystallin methionine residue to methonine sulfoxide, tryptophan to hydroxytryptophan, and N-formylkynurenine [33] and aspartic acid residues at positions 68 and 151 to D-β, D-α, and L-β-aspartic acid

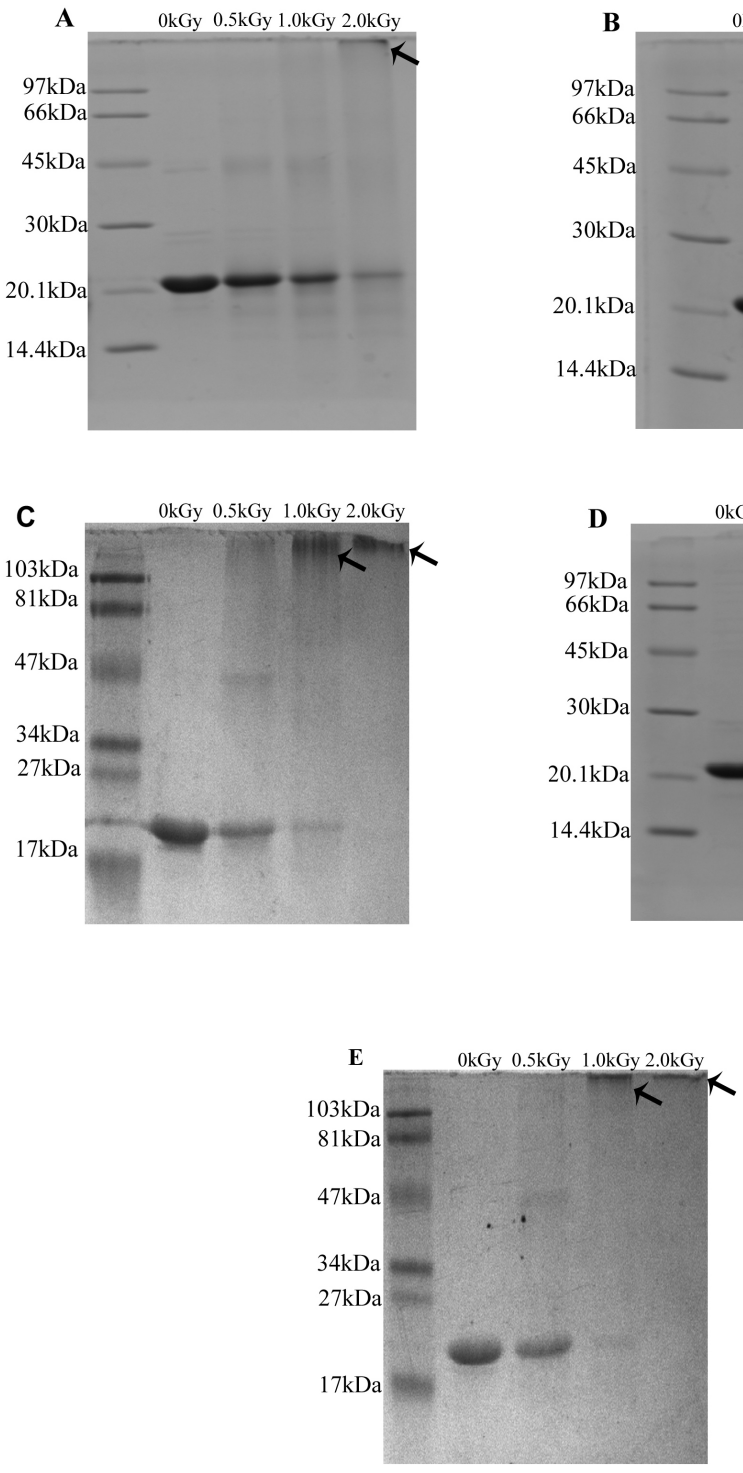

Figure 3. Cross-linked products of αA-crystallin wild-type and N-terminal mutants produced by gamma irradiation. The 15% sodium dodecyl sulfate–polyacrylamide gel electrophoresis (SDS–PAGE) results show the cross-linked products produced by the αA-crystallin wild-type (wt) and N-terminal mutants in non-gamma irradiation (NGI) and after gamma irradiation (GI) with 0.5 kGy, 1.0 kGy, and 2.0 kGy dosages. **A**: αA-crystallin wt exhibited a gradual decrease in monomeric form due to GI and a slight increase in high molecular weight (HMW) cross-linked product at 2.0 kGy. In the case of the mutants, HMW cross-linked products were observed at 1.0 and 2.0 kGy. (**B**) R12C, (**C**) R21L. **D**) R49C, and (**E**) R54C.

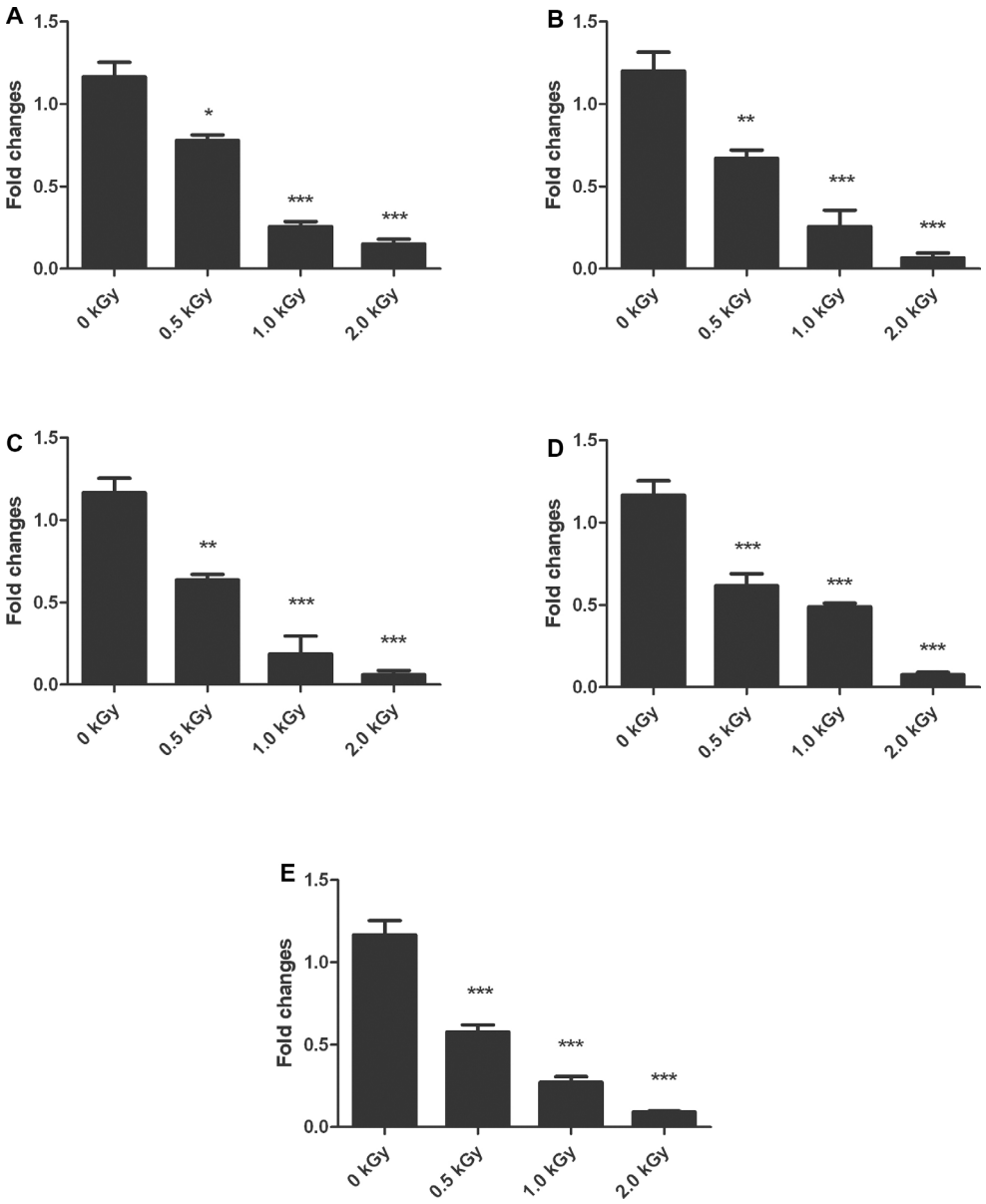

Figure 4. Densitometric analysis of the cross-linked product formed by gamma irradiation (GI) αA-crystallin wild-type and N-terminal mutants. The bar diagram represents the densitometric analysis of the cross-linked product at different dosages of 0, 0.5, 1.0, and 2.0 kGy formed by GI: (**A**) αA-crystallin wild-type (wt), (**B**) R12C, (**C**) R21L, (**D**) R49C, and (**E**) R54C. Each bar represents the mean±standard deviation (SD) of three experiments. *p<0.05, **p<0.01, *** p<0.001 (compared to lane 1 in each case).

[34]. However, little is known about the effect of oxidation on the structural and functional parameters of N-terminal mutants; thus, this study is the first of its kind.

An intriguing finding of the present study is that the αA-crystallin N-terminal mutants (R12C, R21L, R49C, and R54C) exhibited altered structural and functional properties even at 0.5 kGy of GI, and significant levels of modification were recorded at 1.0 kGy and 2.0 kGy exposure. The effect of GI on the oligomeric size of the αA-crystallin wt and N-terminal mutants examined with size exclusion high-performance liquid chromatography (HPLC) demonstrated an increase in the heterogeneity of aggregation in the R12C, R49C, and R54C mutants compared to the NGI mutant counterparts. Significantly, the mutant R21L was resistant to GI at low dosages and showed meager notable aggregation only at 2.0 kGy of GI exposure. It was ascertained that the αA-crystallin N-terminal mutants were more sensitive to GI as a result of changes in the native structure leading to the formation of HMW aggregates as described earlier [35-37]. There was an increase in the aggregation size of the GI N-terminal mutants, since the N-terminal domain maintains the oligomeric size of αA-crystallin [38], a mutation in this domain may make the protein more prone to oxidation. The formation of HMW aggregates as a result of GI may be due to the formation of inter-or intrapeptide cross-linking or hydrophobic as well as disulfide bond (S-S) formation by the amino

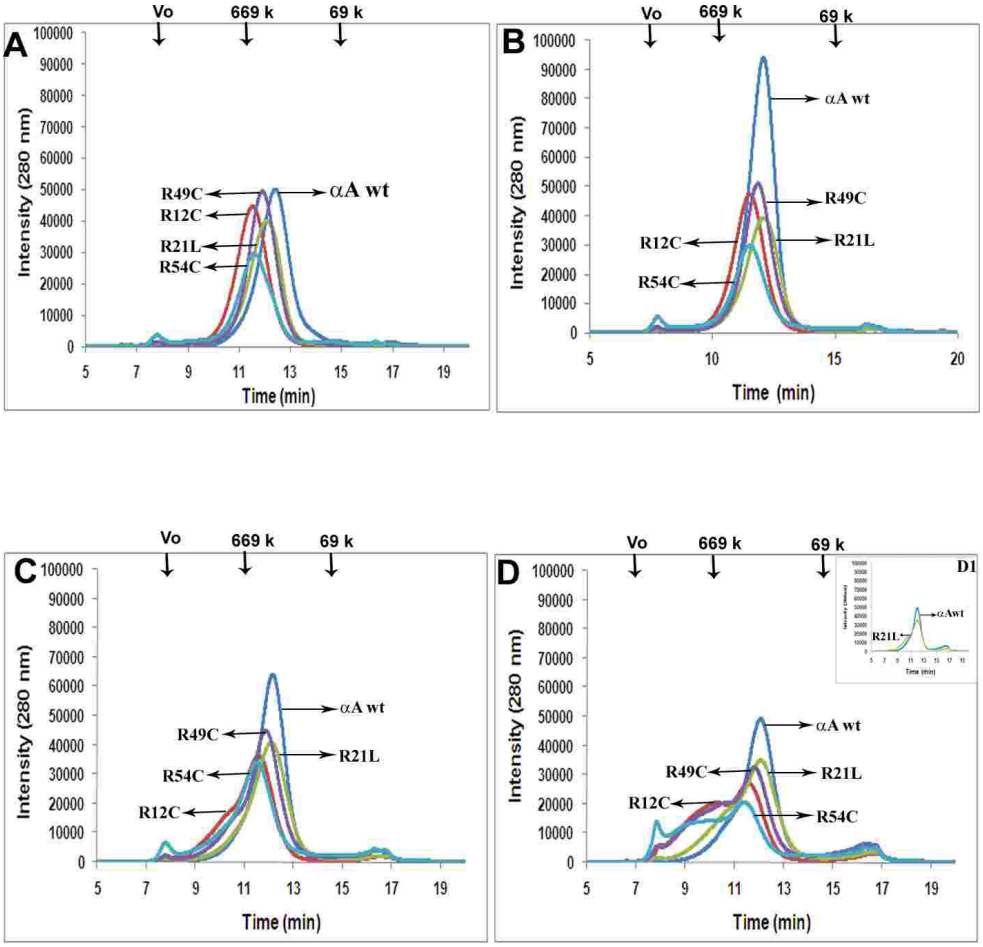

Figure 5. High-performance liquid chromatography–size exclusion profile of gamma ray irradiated αA-crystallin wild-type and N-terminal mutants. The high-performance liquid chromatography (HPLC)–size exclusion chromatographic (SEC) analysis of αA-crystallin wild-type (wt) and N-terminal mutants NGI (**A**) and gamma irradiation (GI) at a dosage of 0.5 kGy (**B**), 1.0 kGy (**C**), and 2.0 kGy (**D**) using the TSKgel-G4000SWXL column. **D1 inset** represents the distinct peaks of αA-crystallin wt and R21L GI at 2.0 kGy. An aliquot of 100 µl of 1 mg/ml protein was injected onto the column, and the elution profile was recorded by absorbance detection at 280 nm. All the non-gamma irradiation (NGI) mutants exhibited slight increased oligomeric size compared to the αA-crystallin wt. The SEC profile at 0.5 kGy shows the slight increased oligomeric size of all mutants compared to wild-type. At 1.0 kGy and 2.0 kGy, all the mutants except R21L demonstrate a notable increase in the aggregate size. Formation of high molecular weight (HMW) aggregates with the profile peak near to the void volume represents the increased aggregate size with an apparent molecular mass of >7 × 10^6 Da. The SEC profile of αA-crystallin wt appears stable in all conditions.

acid radical formed within a peptide chain with the amino radical in another peptide [16,39-42]. Moreover, the size exclusion HPLC findings demonstrate that mutant proteins that have more cysteine residue enhance the formation of HMW aggregate eventually contributing to lens opacification thus leading to scattering of the light. However, αA-crystallin wt and R21L were relatively stable up to 1.0 kGy although a slight increase in aggregate size was observed on exposure at 2.0 kGy.

ROS-induced oxidation results in the disruption of amino acid residue side chains, cleavage of peptide bonds, and formation of covalent protein–protein cross-linked derivatives [43]. In this study, the ROS generated by GI at a low dosage of 0.5 kGy displayed a slight breakdown in the polypeptide chain as revealed in the SDS–PAGE analysis. It increased significantly when exposed to higher dosages. At 1.0 kGy exposure, all the N-terminal mutant proteins were aggregated such that they were unable to penetrate the separating gel. The high amount of cross-linked product formation in the N-terminal mutants revealed their increased susceptibility to ROS-induced oxidation compared to the αA-crystallin wt. Moreover, the sulfur-containing and aromatic amino acids react highly with free radicals compared to aliphatic amino acids [44]. The aromatic amino acid tyrosine is highly sensitive to free radicals leading to hydrogen abstraction resulting in the formation of tyrosyl (phenoxyl) radicals and readily reacts with other tyrosyl molecules to form bityrosine [45]. The intermolecular bityrosine is the mechanism behind the protein aggregation in addition to other cross-links of the proteins [40]. Our results are in line with previous reports that radiolysis of protein extends to form protein–protein cross-linking through tyrosine-tyrosine and nondisulfide cross-links [46]. Eventually, at a high dosage of 2.0 kGy, the increased molecular weight of the mutant proteins was

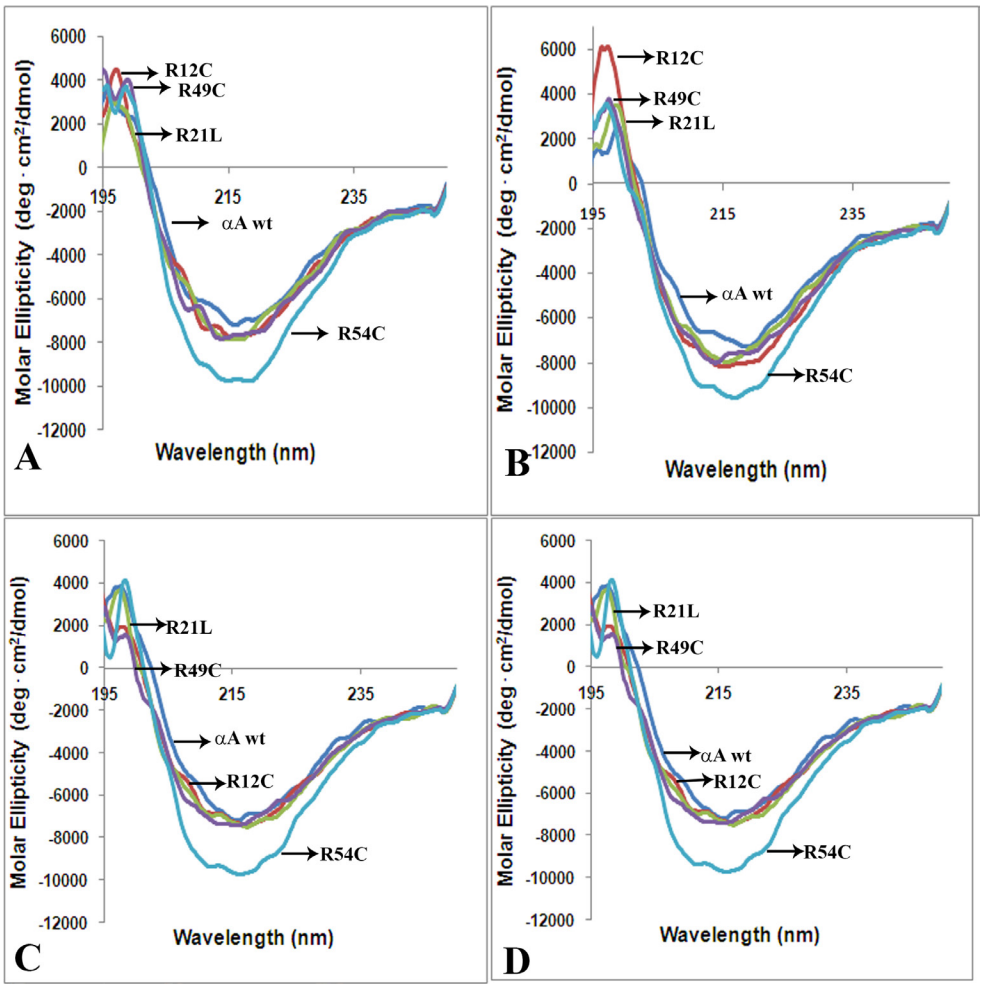

Figure 6. Far ultraviolet circular dichroism spectroscopy. The far ultraviolet circular dichroism (UV–CD) spectra of gamma irradiation and non-gamma irradiation αA-crystallin wild-type and N-terminal mutants, R12C, R21L, R49C, and R54C, were determined with CD spectroscopy. The secondary structure profile of the αA-crystallin wild-type (wt) and N-terminal mutants was evaluated at (**A**) 0 kGy, (**B**) 0.5 kGy, (**C**) 1.0 kGy, and (**D**) 2.0 kGy dosages of GI. The secondary structure profile of the gamma irradiated (GI) αA-crystallin wt was stable at different dosages. However, significant changes in the β-sheet and random coil content in the GI mutants, R12C, R21L, and R49C, was observed at 0.5 kGy. The mutant R54C exhibited changes in β-sheet content only after 1.0 kGy of GI. Each spectrum is an average of five runs. The spectra were recorded between 195 and 250 nm.

found indicating the formation of cross-linked products of the degraded protein molecules [42].

Furthermore, GI of the αA-crystallin N-terminal mutants resulted in significant changes in the secondary structural properties with changes in the β-sheet as well as random coil structural conformation, relative to the NGI counterparts. In contrast, the αA-crystallin wt almost retained its secondary structural integrity up to 2.0 kGy of GI, which is consistent with our previous report, in which GI up to 4.0 kGy did not affect the secondary structure of the αA-crystallin wt [24]. As shown in Figure 6, irradiation affected the CD spectrum of the mutant protein disrupting its fold. Irradiation primarily decreased the ordered structure of the mutant proteins, which resulted in an altered β-sheet structure with a concomitant increase in the random coil content. This shows that the secondary structure of the αA-crystallin N-terminal mutants is more sensitive to gamma rays. The change in the secondary structure is attributed to the breakdown of the covalent bonds and the disruption of the ordered structure of proteins [42,47] finally altering the native function of the protein. The bis-ANS assay results demonstrate that the GI N-terminal mutants R12C and R54C exhibited unusual behavior in exposing hydrophobic patches to the environment. At 0.5 kGy, the mutants R21L and R54C exhibited decreased surface hydrophobicity retaining the same on exposure to 1.0 kGy; however, at 2.0 kGy, R54C demonstrated significant increased fluorescence, and R21L demonstrated decreased fluorescence. R49C in contrast to the other mutants exhibited a slight decrease in surface hydrophobicity at 1.0 and 2.0 kGy. Our results are in contrast to earlier reports that demonstrated in vitro treatment of purified proteins with radiolytically generated hydroxyl radicals leads to an increase in hydrophobicity [39,40,48]. In this study, we have reported a substantial increase in hydrophobicity at low dosage and a decrease at higher dosage upon gamma irradiation of αA-crystallin N-terminal mutants. A plausible explanation for the discrepancy could be that the presence of the mutations in different regions of the N-terminal domain results in different behavior

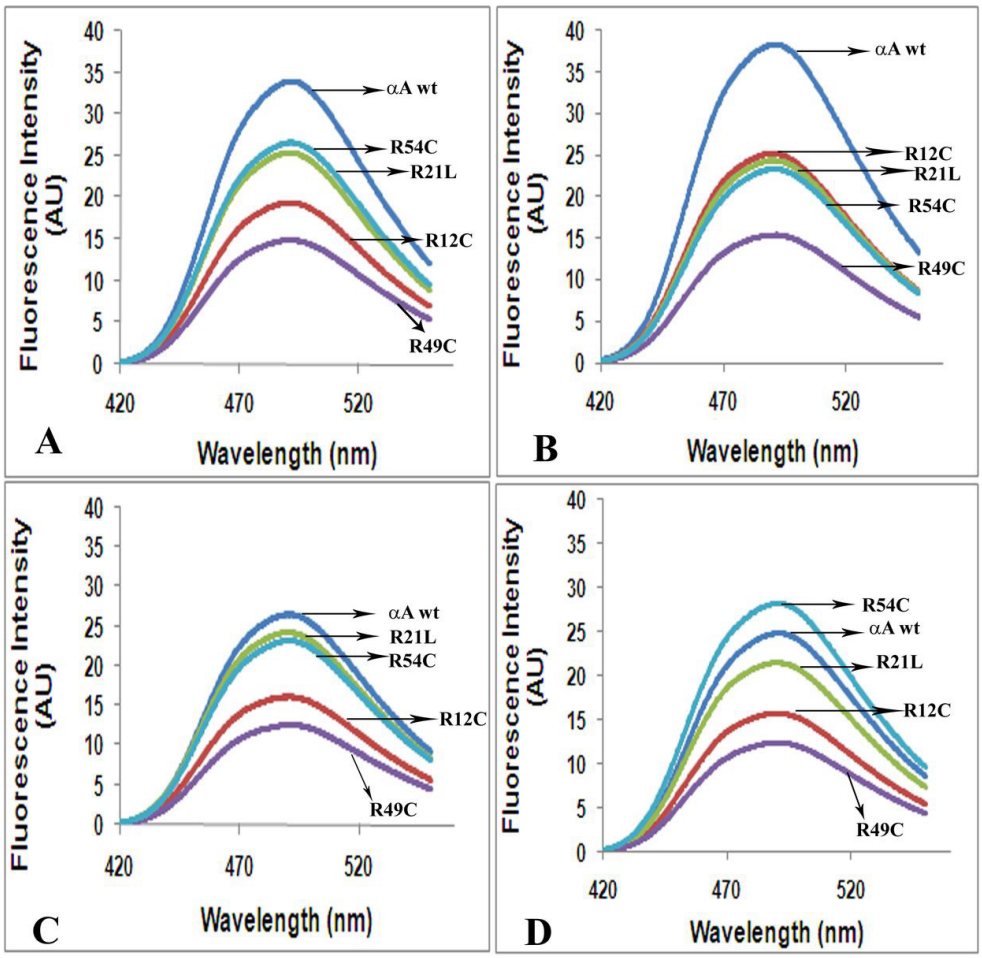

Figure 7. Surface hydrophobicity of the gamma irradiation and non-gamma irradiation αA-crystallin wild-type and its N-terminal mutants. Higher 4,4'-bis(1-anilinonaphthalene 8-sulfonate) (bis-ANS) fluorescence intensity at room temperature shows that the αA-crystallin N-terminal mutants expose hydrophobic patches on the surface upon gamma irradiation (GI). The bis-ANS fluorescence intensity of the αA-crystallin wt and N-terminal mutants was recorded at (**A**) 0 kGy, (**B**) 0.5 kGy, (**C**) 1.0 kGy, and (**D**) 2.0 kGy dosages of GI. At 0 kGy, all mutants exhibited decreased surface hydrophobicity when compared to the αA-crystallin wt. On GI at 0.5 kGy, a slight increase in the surface hydrophobicity was observed for αA-crystallin wt and mutant R12C; however, a slight decrease was observed in the mutants R21L and R54C. At 1.0 kGy, αA-crystallin wt and mutant R12C exhibited a considerable decrease in surface hydrophobicity, no change in R21L, and a slight decrease in R49C. The mutant R54C exhibited a significant increase in surface hydrophobicity at 2.0 kGy, but the other mutants exhibited similar fluorescence as observed at 1.0 kGy.

and characteristics, and thus, we would not expect all mutants to undergo all expected changes [16]. Taking into account the size exclusion, SDS–PAGE, surface hydrophobicity as well as CD experimental results, we concluded that gamma irradiation markedly affects the structural characteristics of all αA-crystallin N-terminal mutants.

Even though there were differences in the exposure of the hydrophobic surface in all mutants after GI, the chaperone activity was increased slightly upon GI revealing that there is no stringent relationship between surface hydrophobicity and the chaperone function in α-crystallin as reported earlier [49,50]. The molecular chaperone function of α-crystallin is known to prevent protein unfolding and aggregation. Many factors including micronutrients are known to have the ability to alter the chaperone function of αA-crystallin [51], although the molecular mechanisms behind the chaperone activity are not completely established. In general, the chaperone activity of αA-crystallin may decrease due to oxidative stress, deamidation, truncation, etc. Since chaperone activity is one of the major functions of αA-crystallin, a reliable and standardized method was used to quantify the chaperone activity of the GI N-terminal mutants in this study. Specifically, EDTA-induced denaturation of ADH was exploited. The major grounds for excluding other substrates such as β_L, γ_D crystallins, and insulin are the highly reproducible outcomes obtained with ADH [16]. An essential criterion in chaperone function is the extent of binding of the chaperone with the substrate. We found that the NGI αA-crystallin wt, mutants R49C and R54C exhibited nearly complete suppression of ADH aggregation whereas the ability was lost in the mutants R12C and R21L corroborating with Kore et al.'s results [16]. However, there was marked elevation in chaperone activity upon oxidation of crystallin protein in all N-terminal mutants relative to NGI counterparts. In particular, the R12C mutant (NGI) lost 50% of chaperone activity due to a mutation as described earlier [16] but showed a fold increase in activity

Table 1. Percentage chaperone activity against EDTA induced aggregation of ADH of gamma irradiated αA-crystallin wt and N-terminal mutants.

Dosage of gamma irradiation (kGy)	Percentage (%) with standard deviation				
	αA-crystallin wt	R12C	R21L	R49C	R54C
0	92.08±4.80	46.77±12.82***	72.36±6.82	87.98±6.66	78.03±7.07
0.5	91.34±5.37	61.45±13.32*	84.60±8.16	93.59±1.01	83.62±10.85
1	89.22±4.50	73.26±2.711*	89.93±3.11	95.91±1.78	85.79±11.30
2	87.91±4.55	80.18±4.02	92.18±0.27	97.41±1.14	88.75±7.31

The values represented as mean ± SD of three individual experiments *p<0.05, *** p<0.001(compared to the αA-crystallin wt).

upon gamma irradiation. We speculated that the increased chaperone activity might be due to changes in hydrophobicity, as a result of oxidation induced by GI, because previously Jang et al. [52] reported a positive correlation between hydrophobicity and chaperone activity. However, we found that in the case of the GI N-terminal mutants of αA-crystallin, hydrophobicity was not always related to chaperone activity as concluded by several other researchers [50,53]. Consequently, gamma ray exposure modifies other physical properties of the mutant proteins rather than hydrophobicity, which increased the chaperone function (yet to be revealed) of the mutated protein [53]. Further, the increase in chaperone activity may be attributed to increased number of cysteine residues at the 12th position involved in disulfide bond formation and covalent protein–protein interaction, which resulted in increased substrate binding potential of the GI mutant proteins. A vibronic transition of chaperone activity in R12C was observed on GI, which shows that this mutant is more

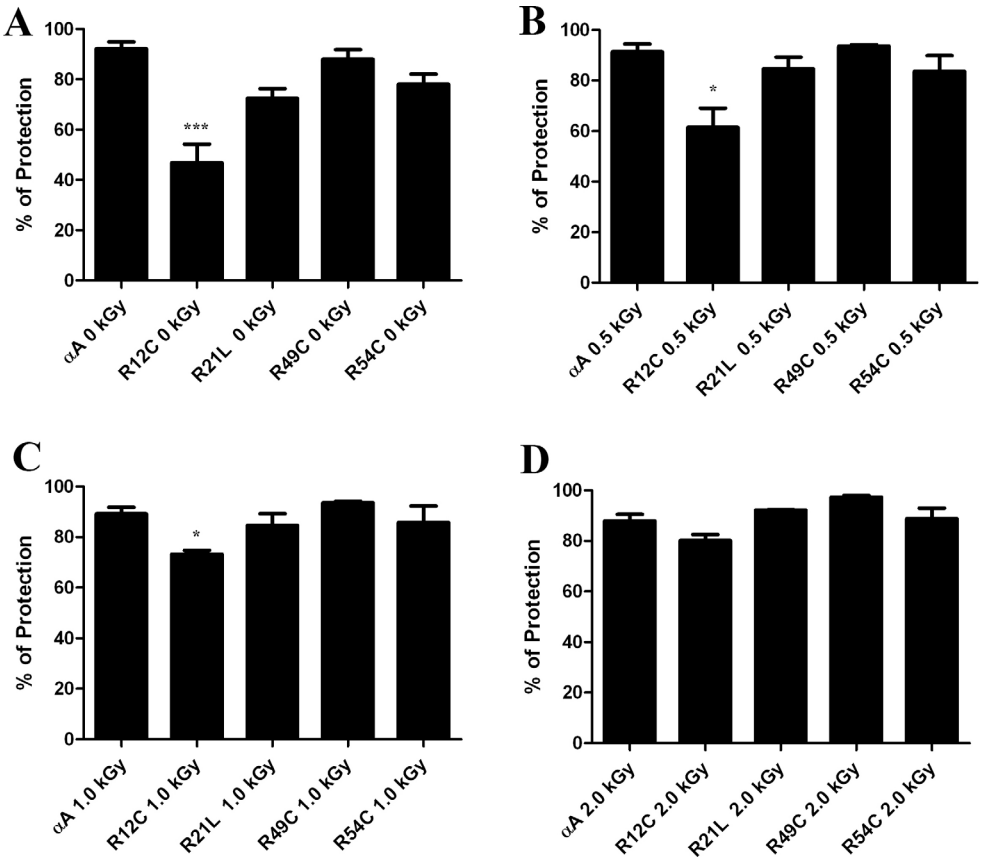

Figure 8. Chaperone activity of gamma irradiated αA-crystallin wild-type and N-terminal mutants. The chaperone activities of non-gamma irradiation (NGI) and gamma irradiation (GI) αA-crystallin wild-type (wt) and N-terminal mutant crystallins were measured by the ability to suppress ethylenediamine tetraacetic acid (EDTA)-induced aggregation of alcohol dehydrogenase (ADH) at a ratio of 1:5. The chaperone activity of αA-crystallin wt and the N-terminal mutants, R12C, R21L, R49C, and R54C, were analyzed at (**A**) 0 kGy, (**B**) 0.5 kGy, (**C**) 1.0 kGy, and (**D**) 2.0 kGy dosages of GI. At 0 kGy, all mutants exhibited decreased chaperone activity compared to αA-crystallin wt. However, a gradual gain of chaperone activity was observed in all mutants on exposure to an increased dosage of GI compared to the NGI mutant counterparts. Each bar represents the mean±standard deviation (SD) of three individual experiments. *p<0.05, ***p<0.001 (compared to lane 1 in each case).

sensitive to oxidation resulting in increased substrate binding potential. However, it is far-fetched to claim that irradiation increases the stability of these mutations because the SDS–PAGE profile, size exclusion chromatogram, and far-UV CD results depict the formation of cross-linked products, large aggregates, and secondary structural alterations. Moreover, it remains questionable whether the gained chaperone function of the protein could prevent the formation of aggregation of other mutant/target proteins or not.

In conclusion, this report analyzed the comparative structural perturbation and functional changes of αA-crystallin wt and its N-terminal mutants in response to gamma irradiation at different dosages. The results demonstrate that an increasing dosage of gamma irradiation resulted in highly altered structural and functional properties of the proteins. High molecular weight cross-linked product formation and aggregation were observed in the mutants exposed to GI reflecting the occurrence of protein oxidation in addition to changes in the surface hydrophobicity pattern. These data clearly indicate that all N-terminal mutants are structurally sensitive to GI. Further, compared with the results of the structural analyses, we speculate that the GI αA-crystallin mutant proteins might have been truncated or oxidized and formed a new complex structure with a changed physical nature that culminated in increased chaperone activity. However, extended studies are needed to elucidate the mechanism by which oxidation induced by GI results in N-terminal mutants' gain in chaperone activity.

ACKNOWLEDGMENTS

The authors gratefully acknowledge the financial assistance from Department of Science and Technology (DST), New Delhi as DST-YS-SR/FT/LS-153/2008/(2010-2013) and DST-JSPS-(DST/INT/JSPS/P-119/ (2011-2013) sanctioned to the corresponding author (Dr. K.A.). The 4th authors thank DST-INSPIRE for senior research fellowship. Authors thank all the anonymous reviewer's for their valuable comments to improve the quality of this manuscript.

REFERENCES

1. Graw J. Genetics of crystallins: cataract and beyond. Exp Eye Res 2009; 88:173-89. [PMID: 19007775].
2. Horwitz J. Alpha-crystallin can function as a molecular chaperone. Proc Natl Acad Sci USA 1992; 89:10449-53. [PMID: 1438232].
3. Alpha-crystallin HJ. Exp Eye Res 2003; 2:145-53. .
4. Biswas A, Goshe J, Miller A, Santhoshkumar P, Luckey C, Bhat MB, Nagaraj RH. Paradoxical effects of substitution and deletion mutation of Arg56 on the structure and chaperone function of human alphaB-Crystallin. Biochemistry 2007; 46:1117-27. [PMID: 17260942].
5. Kuszak JR, Zoltoski RK, Sivertson C. Fibre cell organization in crystalline lenses. Exp Eye Res 2004; 78:673-87. [PMID: 15106947].
6. Devi RR, Yao W, Vijayalakshmi P, Sergeev YV, Sundaresan P, Hejtmancik JF. Crystallin gene mutations in Indian families with inherited pediatric cataract. Mol Vis 2008; 14:1157-70. [PMID: 18587492].
7. Santana A, Waiswol M, Arcieri ES, Cabral de Vasconcellos JP, Barbosa de Melo M. Mutation analysis of CRYAA, CRYGC, and CRYGD associated with autosomal dominant congenital cataract in Brazilian families. Mol Vis 2009; 15:793-800. [PMID: 19390652].
8. Kondo Y, Saitsu H, Miyamoto T, Lee BJ, Nishiyama K, Nakashima M, Tsurusaki Y, Doi H, Miyake N, Kim JH, Yu YS, Matsumoto N. Pathogenic mutations in two families with congenital cataract identified with whole-exome sequencing. Mol Vis 2013; 19:384-9. [PMID: 23441109].
9. Churchill A, Graw J. Clinical and experimental advances in congenital and paediatric cataracts. Philos Trans R Soc Lond B Biol Sci 2011; 366:1234-49. [PMID: 21402583].
10. Haargaard B, Wohlfahrt J, Fledelius HC, Rosenberg T, Melbye M. A nationwide Danish study of 1027 cases of congenital/infantile cataracts: etiological and clinical classifications. Ophthalmology 2004; 111:2292-8. [PMID: 15582089].
11. Hejtmancik JF. Congenital cataracts and their molecular genetics. Semin Cell Dev Biol 2008; 19:134-49. [PMID: 18035564].
12. Fu L, Liang JJ-N. Detection of protein-protein interactions among lens crystallins in a mammalian two-hybrid system assay. J Biol Chem 2002; 277:4255-60. [PMID: 11700327].
13. Hansen L, Yao W, Eiberg H, Kjaer KW, Baggesen K, Hejtmancik JF, Rosenberg T. Genetic heterogeneity in microcornea-cataract: five novel mutations in CRYAA, CRYGD, and GJA8. Invest Ophthalmol Vis Sci 2007; 48:3937-44. [PMID: 17724170].
14. Graw J, Klopp N, Illig T, Preising MN, Lorenz B. Congenital cataract and macular hypoplasia in humans associated with a de novo mutation in CRYAA and compound heterozygous mutations in P. Graefes Arch Clin Exp Ophthalmol 2006; 244:912-9. [PMID: 16453125].
15. Mackay DS, Andley UP, Shiels A. Cell death triggered by a novel mutation in the alphaA-crystallin gene underlies autosomal dominant cataract linked to chromosome 21q. Eur J Hum Genet 2003; 11:784-93. [PMID: 14512969].
16. Kore R, Hedges RA, Oonthonpan L, Santhoshkumar P, Sharma KK, Abraham EC. Quaternary structural parameters of the congenital cataract causing mutants of αA-crystallin. Mol Cell Biochem 2012; 362:93-102. [PMID: 22045060].
17. van den IJssel P, Norman DG, Quinlan RA. Molecular chaperones: Small heat shock proteins in the limelight. Curr Biol 1999; 9:R103-5. [PMID: 10021375].

18. Bera S, Abraham EC. The alphaA-crystallin R116C mutant has a higher affinity for forming heteroaggregates with alphaB-crystallin. Biochemistry 2002; 41:297-305. [PMID: 11772029].

19. Raju I, Abraham EC. Congenital cataract causing mutants of αA-crystallin/sHSP form aggregates and aggresomes degraded through ubiquitin-proteasome pathway. PLoS ONE 2011; 6:e28085-[PMID: 22140512].

20. Raju I, Oonthonpan L, Abraham EC. Mutations in human αA-crystallin/sHSP affect subunit exchange interaction with αB-crystallin. PLoS ONE 2012; 7:e31421-[PMID: 22347476].

21. Raju I, Kannan K, Abraham EC. FoxO3a serves as a biomarker of oxidative stress in human lens epithelial cells under conditions of hyperglycemia. PLoS ONE 2013; 8:e67126-[PMID: 23805295].

22. Anbarasu K. Srinivasagan Ramkumar, Bency Thankappan, Abraham EC. Towards to clarify the etiology of cataract by crystallin protein-protein interaction studies. JSCRS 2013; 25:67-74. .

23. Fujii N, Nakamura T, Sadakane Y, Saito T, Fujii N. Differential susceptibility of alpha A- and alpha B-crystallin to gamma-ray irradiation. Biochim Biophys Acta 2007; xxx:345-50. .

24. Fujii N, Hiroki K, Matsumoto S, Masuda K, Inoue M, Tanaka Y, Awakura M, Akaboshi M. Correlation between the loss of the chaperone-like activity and the oxidation, isomerization and racemization of gamma-irradiated alpha-crystallin. Photochem Photobiol 2001; 74:477-82. [PMID: 11594064].

25. Laemmli UK. Cleavage of structural proteins during the assembly of the head of bacteriophage T4. Nature 1970; 227:680-5. [PMID: 5432063].

26. Takemoto L, Emmons T. Truncation of alpha A-crystallin from the human lens. Exp Eye Res 1991; 53:811-3. [PMID: 1783018].

27. Emmons T, Takemoto L. Age-dependent loss of the C-terminal amino acid from alpha crystallin. Exp Eye Res 1992; 55:551-4. [PMID: 1483501].

28. Takemoto L, Horwitz J, Emmons T. Oxidation of the N-terminal methionine of lens alpha-A crystallin. Curr Eye Res 1992; 11:651-5. [PMID: 1521466].

29. Fujii N, Satoh K, Harada K, Ishibashi Y. Simultaneous stereoinversion and isomerization at specific aspartic acid residues in alpha A-crystallin from human lens. J Biochem 1994; 116:663-9. [PMID: 7852288].

30. Fujii N, Ishibashi Y, Satoh K, Fujino M, Harada K. Simultaneous racemization and isomerization at specific aspartic acid residues in alpha B-crystallin from the aged human lens. Biochim Biophys Acta 1994; 1204:157-63. [PMID: 8142454].

31. Miesbauer LR, Zhou X, Yang Z, Sun Y, Smith DL, Smith JB. Post-translational modifications of water-soluble human lens crystallins from young adults. J Biol Chem 1994; 269:12494-502. [PMID: 8175657].

32. Kumarasamy A, Abraham EC. Interaction of C-terminal truncated human alphaA-crystallins with target proteins. PLoS ONE 2008; 3:e3175-[PMID: 18779867].

33. Finley EL, Dillon J, Crouch RK, Schey KL. Radiolysis-induced oxidation of bovine alpha-crystallin. Photochem Photobiol 1998; 68:9-15. [PMID: 9679446].

34. Aki K, Fujii N, Fujii N. Kinetics of isomerization and inversion of aspartate 58 of αA-crystallin peptide mimics under physiological conditions. PLoS ONE 2013; 8:e58515-[PMID: 23505525].

35. Stevens CO, Sauberlich HE, Bergstrom GR. Radiation-produced aggregation and inactivation in egg white lysozyme. J Biol Chem 1967; 242:1821-6. [PMID: 6024772].

36. Huang L, Grim S, Smith LE, Kim PM, Nickoloff JA, Goloubeva OG, Morgan WF. Ionizing radiation induces delayed hyperrecombination in Mammalian cells. Mol Cell Biol 2004; 24:5060-8. [PMID: 15143196].

37. Jedziniak JA, Kinoshita JH, Yates EM, Hocker LO, Benedek GB. On the presence and mechanism of formation of heavy molecular weight aggregates in human normal and cataractous lenses. Exp Eye Res 1973; 15:185-92. [PMID: 4692231].

38. Kundu M, Sen PC, Das KP. Structure, stability, and chaperone function of alphaA-crystallin: role of N-terminal region. Biopolymers 2007; 86:177-92. [PMID: 17345631].

39. Davies KJ, Delsignore ME. Protein damage and degradation by oxygen radicals. III. Modification of secondary and tertiary structure. J Biol Chem 1987; 262:9908-13. [PMID: 3036877].

40. Davies KJ, Lin SW, Pacifici RE. Protein damage and degradation by oxygen radicals. IV. Degradation of denatured protein. J Biol Chem 1987; 262:9914-20. [PMID: 3036878].

41. Le Maire M, Thauvette L, de Foresta B, Viel A, Beauregard G, Potier M. Effects of ionizing radiations on proteins. Evidence of non-random fragmentations and a caution in the use of the method for determination of molecular mass. Biochem J 1990; 267:431-9. [PMID: 2334402].

42. Lee Y, Song K. Bin. Effect of gamma-irradiation on the molecular properties of myoglobin. J Biochem Mol Biol 2002; 35:590-4. [PMID: 12470593].

43. Stadtman ER, Berlett BS. Reactive oxygen-mediated protein oxidation in aging and disease. Chem Res Toxicol 1997; 10:485-94. [PMID: 9168245].

44. Thakur BR, Singh RK. Food irradiation chemistry and applications. Food Rev Int 1994; 10:437-73. .

45. Prütz WA, Butler J, Land EJ. Phenol coupling initiated by one-electron oxidation of tyrosine units in peptides and histone. Int J Radiat Biol Relat Stud Phys Chem Med 1983; 44:183-96. [PMID: 6603438].

46. Stadtman ER. Oxidation of free amino acids and amino acid residues in proteins by radiolysis and by metal-catalyzed reactions. Annu Rev Biochem 1993; 62:797-821. [PMID: 8352601].

47. Moon S, Song K. Bin. Effect of γ-irradiation on the molecular properties of ovalbumin and ovomucoid and protection by ascorbic acid. Food Chem 2001; 74:479-83. .

48. Pacifici RE, Kono Y, Davies KJ. Hydrophobicity as the signal for selective degradation of hydroxyl radical-modified hemoglobin by the multicatalytic proteinase complex, Proteasome. J Biol Chem 1993; 268:15405-11. [PMID: 8393440].

49. Bhattacharyya J, Srinivas V, Sharma KK. Evaluation of hydrophobicity versus chaperonelike activity of bovine alpha A- and alpha B-crystallin. J Protein Chem 2002; 21:65-71. [PMID: 11902669].

50. Reddy GB, Kumar PA, Kumar MS. Chaperone-like activity and hydrophobicity of alpha-crystallin. IUBMB Life 2006; 58:632-41. [PMID: 17085382].

51. Reddy GB, Reddy PY, Vijayalakshmi A, Kumar MS, Suryanarayana P, Sesikeran B. Effect of long-term dietary manipulation on the aggregation of rat lens crystallins: role of alpha-crystallin chaperone function. Mol Vis 2002; 8:298-305. [PMID: 12193883].

52. Jang HH, Kim SY, Park SK, Jeon HS, Lee YM, Jung JH, Lee SY, Chae HB, Jung JY, Lee KO, Lim CO, Chung WS, Bahk JD, Yun DJ, Cho MJ, Lee SY. Phosphorylation and concomitant structural changes in human 2-Cys peroxiredoxin isotype I differentially regulate its peroxidase and molecular chaperone functions. FEBS Lett 2006; 580:351-5. [PMID: 16376335].

53. An BC, Lee SS, Lee JT, Park C-H, Lee SY, Chung BY. Change in the enzymatic dual function of the peroxiredoxin protein by gamma irradiation. Radiat Phys Chem 2012; 81:1136-40. .

Articles are provided courtesy of Emory University and the Zhongshan Ophthalmic Center, Sun Yat-sen University, P.R. China. The print version of this article was created on 7 July 2014. This reflects all typographical corrections and errata to the article through that date. Details of any changes may be found in the online version of the article.